AS1.579, the initial inoculum concentration was about 0.1 $OD_{600\ nm}$ in 10 mL MRS medium, and cells were grown at 37 °C for 4 h to reach an optical density at 0.8 $OD_{600\ nm}$. Basically, for RNA isolation, the cells were collected from 10 mL cultures by centrifugation at 4,000 × g for 5 min at 4 °C. A guanidine thiocyanate method was modified by adding a pre-warm step of lysis buffer. In brief, the cells were washed once by 1 mL prechilled PBS (137 mM NaCl, 2.7 mM KCl, 10 mM Na_2HPO_4, 2 mM KH_2PO_4, pH 7.4). Cells were suspended in 500 μL TE buffer (10 mM Tris-HCl, 1 mM EDTA, 10 mM lysozyme, 10 mM DTT, and 37 °C) for 30 min. Fifty units of proteinase K was added and incubated at 65 °C for 30 min. 100 μL 5 M NaCl, 100 μL CTAB was added and incubated at 65 °C for 10 min. Finally, 500 μL phenol/chloroform/isoamyl alcohol (24:24:1, v/v/v, pre-warmed to 60 °C) were added orderly and mixed. The mixture was vortexed vigorously for 30 s and cooled on ice for 15 min, followed by centrifugation at 15,000 × g for 10 min at 4 °C. To precipitate RNA, the aqueous phase was transferred to a 1.5 mL RNase-free Eppendorf tube, mixed with an equal volume pre-chilled isopropanol and stored at −20 °C for 2 h. The RNA pellet was collected by centrifugation at 10,000 × g for 15 min at 4 °C and washed twice with 75% (v/v) ethanol, air dried and dissolved in 10 μL RNase-free water. The isolated small RNA was viewed using 1% agarose gel electrophoresis.

Following the washing treatment, the competitive absorbtion for sepiolite between DNA and RNA was tested. Ten milligrams precipitated sepiolite was added to 10 μL 300 ng/μL RNA and mixed completely. Meanwhile, the control group was carried out: Ten milligrams precipitated sepiolite was added to 10 μL 400 mM Guanidine Hydrochloride (pH 4.0) and mixed completely. The supernatant was transferred into a 200-μL microtube after centrifugation. The DNA was precipitated with 75% ethanol and dissolved in 5 μL TE. All the samples were checked using 1% agarose gel electrophoresis.

The effect of the addition of RNA to the plasmid transformation was performed as following: 50 μL of transforming mixture consisting of 50 μL LB, bacteria ($OD_{600\ nm} = 20$), 1% sepiolite, 300 ng (or 3 μg) RNA and 100 ng pET15b were transferred into a 500-μL microtube (DNA is added in the end); the mixture was resuspended in a vortex mixer by mixing at full speed for 1 min; and then the cells were spread on a 1% agar plate with 100 μg/mL ampicillin and incubated at 37 °C overnight.

Finally, the effect of the degree of richness of the sepiolite fibers on the plasmid transformation was considered. For this purpose, 500 mg of sepiolite was suspended in 50 mL sterile water and mixed thoroughly. The sepiolite suspension was placed at room temperature for 2 h, and the supernatant was transferred into a new tube and collected through centrifugation at 5,000 × g for 2 min. The precipitation was suspended in 25 mL sterile water as sepiolite 2. Two hundred milligrams of sepiolite was suspended in 20 mL sterile water and ultrasonicated at 200 W for 2 min. The ultrasonicated sepiolite was regarded as sepiolite 3 and untreated sepiolite was named as sepiolite 1. Finally, 1 mg/mL of GFPuv was added to the sepiolite 1, 2 and 3 and mixed thoroughly. After absorbing GFPuv, the shape of the sepiolite was observed under a fluorescence microscope (Nikon TE2000, Nikon Corporation, Tokyo, Japan). Using the three kinds of sepiolites, plasmid transformation was performed as above mentioned and compared.

4. Conclusions

Using nanomaterials—based on the Yoshida effect—can make DNA transformation rapid and simple. However, the amount of 0.01% nanomaterials (w/v) presented previously is too low to be

successful for bacterial transformation. We used 0.1% nanomaterials (w/v) to achieve enhanced transformation efficiency by approximately 100-fold. Based on the new result, vortex operation would be better than streaking a plate in a single continuous movement to further enhance the transformation up to almost 10-fold. Meanwhile, for such a transformation, there may be an alternative mechanism to explain our findings.

Acknowledgements

We would like to thank Gottfried Wilharm for providing the information for obtaining sepiolite. The financial supports of National Basic Research Program of China (973 Program) (No. 2007CB707802), National Natural Science Foundation of China (Key Program, Grant No. 30930038) and the Japanese Ministry of Education, Science, Sports and Culture, Grant-in-Aid for Scientific Research (B) No. 21300179 are gratefully acknowledged.

References

1. Yoshida, N.; Ikeda, T.; Yoshida, T. Chrysotile asbestos fibers mediate transformation of *Escherichia coli* by exogenous plasmid DNA. *FEMS Microbiol. Lett.* **2001**, *195*, 133–137.
2. Landrigan, P.J.; Nicholson, W.J.; Suzuki, Y. The hazards of chrysotile asbestos: a critical review. *Ind. Health* **1999**, *37*, 271–280.
3. Yoshida, N.; Ide, K. Plasmid DNA is released from nanosized acicular material surface by low molecular weight oligonucleotides: exogenous plasmid acquisition mechanism for penetration intermediates based on the Yoshida effect. *Appl. Microbiol. Biotechnol.* **2008**, *80*, 813–821.
4. Wilharm, G.; Lepka, D.; Faber, F. A simple and rapid method of bacterial transformation. *J. Microbiol. Method* **2010**, *80*, 215–216.
5. Yoshida, N.; Sato, M. Plasmid uptake by bacteria: a comparison of methods and efficiencies. *Appl. Microbiol. Biotechnol.* **2009**, *83*, 791–798.
6. Zhang, Z.; Shen, C.; Wang, M.; Han, H.; Cao, X. Aqueous suspension of carbon nanotubes enhances the specificity of long PCR. *Biotechniques* **2008**, *44*, 537–545.
7. Rojas-Chapana, J.; Troszczynska, J.; Firkowska, I. Multi-walled carbon nanotubes for plasmid delivery into *Escherichia coli* cells. *Lab. Chip* **2005**, *5*, 536–539.
8. Sung, K.; Khan, S.A.; Nawaz, M.S. A simple and efficient Triton X-100 boiling and chloroform extraction method of RNA isolation from Gram-positive and Gram-negative bacteria. *FEMS Microbiol. Lett.* **2003**, *229*, 97–101.
9. Joshi, R.P.; Schoenbach, K.H. Mechanism for membrane electroporation irreversibility under high-intensity, ultrashort electrical pulse conditions. *Phys. Rev. E* **2002**, *66*, 052901.
10. Yoshida, N. Discovery and application of the Yoshida effect: Nano-sized acicular materials enable penetration of bacterial cells by sliding friction force. *Rec. Pat. Biotechnol.* **2007**, *1*, 194–201.
11. Yoshida, N.; Saeki, Y. Chestnut bur-shaped aggregates of chrysotile particles enable inoculation of *Escherichia coli* cells with plasmid DNA. *Appl. Microbiol. Biotechnol.* **2004**, *65*, 566–575.
12. Yoshida, N.; Kodama, K.; Nakata, K. *Escherichia coli* cells penetrated by chrysotile fibers are transformed to antibiotic resistance by incorporation of exogenous plasmid DNA. *Appl. Microbiol. Biotechnol.* **2002**, *60*, 461–468.

13. Yoshida, N.; Nakajima-Kambe, T.; Matsuki, K. Novel plasmid transformation method mediated by chrysotile, sliding friction, and elastic body exposure. *Anal. Chem. Insights* **2007**, *2*, 9–15.
14. Tu, Z.; He, G.; Li, K. An improved system for competent cell preparation and high efficiency plasmid transformation using different *Escherichia coli* strains. *Electron. J. Biotechnol.* **2005**, *8*, 113–120.

plant disease

November 2010, Volume 94, Number 11
Page 1378
DOI: 10.1094/PDIS-07-10-0549

Disease Notes

First Report of *Cucumber mosaic virus* in Sweet Cherry in the People's Republic of China

H. D. Tan, **S. Y. Li**, and **X. F. Du**, Dalian Institute of Biotechnology, Liaoning Academy of Agricultural Sciences, Dalian 116023, People's Republic of China; and **M. Seno**, Department of Medical and Bioengineering Science Graduate School of Natural Science and Technology, Okayama University, Okayama 700-8530, Japan

From the spring of 2003 to the summer of 2006, sweet cherry (*Prunus avium*) trees in orchards near Lvshun City, in the northeast People's Republic of China, had symptoms suggestive of those caused by *Cucumber mosaic virus* (CMV; genus *Cucumovirus*, family *Bromoviridae*). Symptoms included chlorotic patches or mottling on leaves that were also deformed (4). In April 2006, 20 symptomatic leaves sampled from 10 trees in each of four orchards were assayed for CMV with a CMV-specific antiserum (Agdia Inc., Elkhart, IN) in a double-antibody sandwich-ELISA. Of the 80 symptomatic leaf samples, 27 tested positive for the presence of CMV. CMV was detected in all four orchards, within which incidence varied between 0.5 and 4%. Viral nucleoproteins were purified by differential centrifugation and sucrose density gradient fractionation from symptomatic leaves. Transmission electron microscopy of nucleoproteins revealed isometric particles approximately 30 nm in diameter, which is also typical of CMV. Total RNA was also extracted from 100 mg of symptomatic tissue following a Trizol-based protocol (1). A reverse transcriptase-PCR assay with nucleocapsid gene-specific primers was then used (forward primer 5′-ATGGCGACGTCCTCGTTCA-3′; reverse primer 5′-CATCGTTCCCTTCAAAATAG-3′) (3). A PCR product of approximately 633 bp was obtained. The PCR product was cloned and sequenced. The sequence (GenBank Accession No. HM996559) had 95% identity with the RNA-1 sequence from CMV 'Fny' strain in GenBank (Accession No. D00356.1). The People's Republic of China is one of the major producers of sweet cherry in Asia and the spread of CMV in China may cause significant economic losses. Thus, virus-infected material should not be used for propagation and surveys should be undertaken to determine if the aphid vectors capable of transmitting CMV are present (2).To our knowledge, this is the first report of CMV occurring in sweet cherry orchards in the People's Republic of China.

References: (1) P. Chomczynski and K. Mackey. Biotechniques 19:942, 1995. (2) F. E. Gildow et al. Phytopathology 98:1233, 2008. (3) T. M. Rizzo and P. Palukaitis. J. Gen. Virol. 70:1, 1989. (4) J. Shang et al. Z. Naturforsch. C 65:73, 2010.

Full Paper

CONTRAST MEDIA & MOLECULAR IMAGING

Received: 15 February 2009, Revised: 7 December 2009, Accepted: 16 December 2009, Published online in Wiley InterScience: 16 March 2010

(www.interscience.wiley.com) DOI:10.1002/cmmi.367

E-selectin targeting to visualize tumors in vivo

Masahiko Hirai[a,b], Yoshie Hiramatsu[a], Shinki Iwashita[a], Takayuki Otani[a,b], Ling Chen[b], Yue-guang Li[b], Masashi Okada[b], Kazunori Oie[a], Koich Igarashi[a], Hideaki Wakita[c] and Masaharu Seno[b]*

Generally angiogenic factors induce the expression of E-selectin in vascular endothelial cells in the tumors. In this study, we employed an anti-E-selectin monoclonal antibody to target tumors *in vivo* and evaluated an optical imaging reagent to visualize tumor regions. The anti-E-selectin antibody was conjugated on the surface of liposomes, which encapsulated the near-infrared fluorescent substances Cy3 or Cy5.5. The liposomes efficiently recognized human umbilical vein endothelial cells only when E-selectin was induced by angiogenic factors such as TNF-α *in vitro*. Cy5.5 encapsulated into liposomes that were conjugated with an anti-E-selectin antibody successfully visualized Ehrlich ascites tumor cells when transplanted into mice. Thus, E-selectin targeting with liposomes containing a near-infrared fluorescent dye was found effective in visualizing tumors *in vivo*. This strategy should be extremely useful as a method to identify sentinel lymphatic nodes and angiogenic tumors as well as use for drug delivery to tumor cells. Copyright © 2010 John Wiley & Sons, Ltd.

Keywords: Liposome; E-selectin; *in vivo* imaging; drug delivery system

1. INTRODUCTION

The field of non-invasive *in vivo* imaging is rapidly growing with new technologies and techniques. Near-infrared fluorescent substances are being utilized for *in vivo* imaging of small animals because the near-infrared region of the spectrum offers certain advantages for photon penetration and because both organic and inorganic fluorescence contrast agents are now available for chemical conjugation to targeting molecules (1). Liposomes are currently being utilized as carriers for delivering various drugs and substances. For passive delivery both the size and electric charge of the surface of liposomes have to be carefully optimized to deliver agents to the proper targets (2–4). Various molecules such as antibodies, transferrin, folic acid and monosaccharide have been conjugated to the surface of liposomes but few have been successful for targeting tumor cells (4,5). Taking this into consideration, we reasoned that the E-selectin ligand might confer potential tumor targeting to liposomes (6,7). E-selectin is expressed on tumor vascular endothelial cells that have been stimulated by cytokines such as TNF-α, IL1-β and VEGF (8–13). While there are 14 lectin categories, which are classified by their primary structure, including C-type lectin, galectin, I-type lectin, P-type lectin and pentraxin (14–16), E-selectin belongs to the C-type lectin family and is well characterized in inflammation and in tumors. Liposomes that have been conjugated with an anti-E-selectin antibody can successfully target cells that are expressing E-selectin *in vitro* (17–20). However, *in vivo* targeting with liposomes conjugated with such an antibody has not been successful because liposomes are rapidly depleted *in vivo* after being entrapped by the reticular endothelial system (RES) in the liver and spleen or by binding to opsonin proteins in blood and then phagocytosed by macrophages (4,5,17). More extended retention in the blood vessels appears to be necessary for binding to endothelial cells on which E-selectin is expressed.

In this report, we describe a method for targeting tumor cells *in vivo* for imaging using a near-infrared fluorescent dye which has been encapsulated into liposomes which are conjugated to anti-E-selectin antibody and which have been negatively charged with a hydrophilic substance.

2. RESULTS

2.1. Properties of liposomes

Cy3 or Cy5.5 encapsulated liposomes were conjugated with anti-E-selectin antibody (Fig. 1). The surface of the liposomes was modified to possess a negative charge so that repulsive forces between the liposomes and the wall of blood vessels would reduce non-specific binding of the liposomes *in vivo*. The final concentration of lipid of the liposomes encapsulating Cy5.5 was in the range from 2.5 to 3.0 mg/ml and the concentration of Cy3 was from 2.7 to 3.1 mg/ml. As summarized in Table 1, the mean particle size of the liposome population was approximately 90 nm, which was not affected by either the type of dye that was encapsulated or the quantity of antibody that was conjugated on

* *Correspondence to: M. Seno, Rm361, Bldg ENG-6, Department of Medical and Bioengineering Science, Graduate School of Natural Science and Technology, Okayama University, 3.1.1 Tsushima-naka, Kita-ku, Okayama 700-8530, Japan. E-mail: mseno@cc.okayama-u.ac.jp*

a *M. Hirai, Y. Hiramatsu, S. Iwashita, T. Otani, K. Oie, K. Igarashi R&D Division, Katayama Chemical Industries Co. Ltd, Minoh, Osaka 562-0015, Japan*

b *M. Hirai, T. Otani, L. Chen, Y.-g. Li, M. Okada, M. Seno Laboratory of Nano-Biotechnology, Department of Medical and Bioengineering Science, Graduate School of Natural Science and Technology, Okayama University, 3.1.1 Tsushima-Naka, Kita-ku, Okayama 700-8530, Japan*

c *H. Wakita Section of Prevention and Therapy, Department of Vascular Dementia Research, National Institute for Longevity Sciences, National Center for Geriatrics and Gerontology, Obu, Aichi 474-8511, Japan*

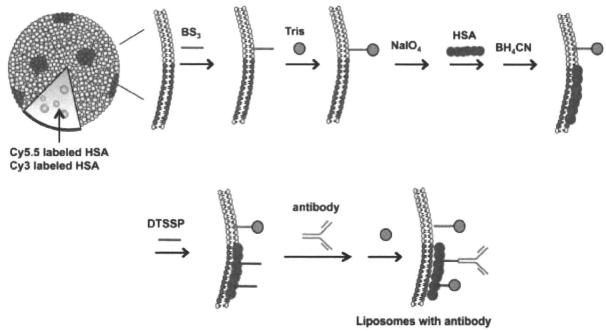

Figure 1. Preparation scheme of liposomes conjugated with antibody. First of all, Cy3 or Cy5.5 conjugated with human serum albumin (HSA) was encapsulated in the hydrophilic anionic liposomes. Then tris(hydroxymethyl)aminomethane (Tris) was crosslinked on the liposomes surface via bis(sulfosuccinimidyl)suberate (BS_3). HSA was bound to the ganglioside component of liposomes. Finally, anti-E-selectin antibody was conjugated to HSA via DTSSP.

the surface. The ζ-potential, which reflects the surface electric charge of the liposome membrane, was approximately −60 mV (Table 1). The size distribution of the liposomes did not show any changes during 6 months of storage at 4°C.

2.2. Concentrations of antibody conjugated to liposomes

Various concentrations of antibody were assessed to optimize the efficiency of conjugation between liposomes and anti-E-selectin antibody (Table 1). The amount of antibody bound to the surface of the liposomes increased depending on the concentration of antibody in the reaction. As described below, the optimal amount of antibody bound to the surface of liposomes was over 3.9 μg/mg lipid for *in vivo* imaging experiments such that the concentration of antibody in the reaction should be approximately 75 μg/mL or more.

2.3. Expression of E-selectin on vascular endothelial cells after treatment with Ehrlich ascites tumor (EAT)-conditioned medium

In vascular endothelial cells, E-selectin is induced by inflammatory cytokines or angiogenic factors such as IL1-β, TNF-α and VEGF where it is not usually expressed (8–13). This induction was confirmed on human umbilical vein endothelial cells (HUVEC) stimulated with TNF-α in serum-free conditions (Fig. 2). Although culture medium containing fetal bovine serum (FBS) did not induce E-selectin expression, the conditioned medium of EAT

Table 1. Physicochemical properties of liposomes conjugated with anti-E-selectin antibody

	Antibody concentration in conjugating reaction (μg/ml)						
	0	25	50	75	100	200	300
Cy5.5 encapsulated liposomes (n = 3)							
Diameter (nm)	82 ± 2	82 ± 4	82 ± 4	91 ± 3	86 ± 4	84 ± 3	86 ± 2
ζ-Potential (mV)	−56 ± 4	−59 ± 4	−58 ± 5	−55 ± 8	−60 ± 8	−49 ± 9	−51 ± 6
Lipid concentration (mg/ml)	2.5 ± 0.2	2.9 ± 0.1	3.0 ± 0.2	2.8 ± 0.1	2.8 ± 0.2	2.7 ± 0.2	2.7 ± 0.2
Absorbance at 680 nm	2.0	1.9	2.2	1.8	1.7	1.6	1.8
Antibody bound to liposomes (μg/mg lipid)	0	1.0 ± 0.2	2.7 ± 0.4	3.9 ± 0.7	4.5 ± 0.6	6.2 ± 0.8	7.6 ± 0.5
Cy3 encapsulated liposomes (n = 3)							
Diameter (nm)	87 ± 4	85 ± 4	89 ± 3	82 ± 2	ND[a]	ND	ND
ζ-Potential (mV)	−60 ± 2	−59 ± 4	−63 ± 5	−52 ± 6	ND	ND	ND
Lipid concentration (mg/ml)	2.8 ± 0.3	3.1 ± 0.1	2.7 ± 0.1	2.9 ± 0.4	ND	ND	ND
Absorbance at 580 nm	2.8	2.5	2.6	2.4	ND	ND	ND
Antibody bound to liposomes (μg/mg lipid)	0	1.2 ± 0.3	2.5 ± 0.5	3.9 ± 0.4	ND	ND	ND

[a]Not determined.

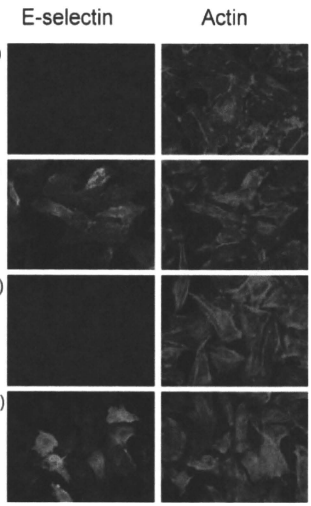

Figure 2. Induction of E-selectin expression in HUVEC. HUVEC were cultured in medium (A), with 10 ng/ml of TNF-α (B), with the fresh medium prepared for EAT cells (C) and with the conditioned medium of EAT cells (D). To detect E-selectin, anti-E-selectin antibody was used followed by FITC labeled anti-mouse IgG antibody. Actin filaments were stained with rhodamine phalloidin. Magnification was × 40.

cells induced the expression of E-selectin in HUVEC, suggesting that EAT cells secretes cytokines or factors stimulating E-selectin expression in HUVEC.

2.4. Visualization of vascular endothelial cells by targeting E-selectin in vitro

Liposomes that had been conjugated to an anti-E-selectin antibody were added to the culture medium of HUVEC that was expressing E-selectin. Since fluoresce of Cy3 is stronger than that of Cy5.5 *in vitro*, liposomes encapsulating Cy3 were used in this experiment. As shown in Fig. 3, HUVEC were visualized by the fluorescent signal of Cy3 only when the liposomes were conjugated with antibody against E-selectin. The specific binding of liposomes to E-selectin was assessed in the presence of an excess amount of free anti-E-selectin antibody. As a result, the fluorescence of liposomes was completely abrogated (Fig. 3C).

2.5. Expression of E-selectin on vascular vessel in EAT

To confirm the expression of E-selectin on vascular vessels in EAT tumor tissues, tumors were excised 10 days after transplantation and tissue sections were prepared, fixed and stained for E-selectin with FITC labeled anti-E-selectin antibody. Additionally, vessels were stained with *Lycopersicon esculentum* (tomato) lectin, which recognizes specifically fucose on the vascular endothelial cells (21). The expression sites of E- selectin staining in the tumor tissue were within the regions of vascular endothelials (Fig. 4). This demonstrates that the expression of E-selectin was induced on blood vessels endothelial cells in EAT tumor tissues. Collectively with the *in vitro* data, these results suggest that EAT cells should secrete cytokines or factors which can induce E-selectin expression in mouse vascular endothelial cells (Fig. 2).

2.6. Visualization of tumors by targeting E-selectin in vivo

To assess if tumor *in vivo* could be visualized, liposomes conjugated with anti-E-selectin antibody in the range from 0 to 7.6 μg antibody/mg lipid of liposome were injected into EAT-bearing mice via the tail vein. Liposomes encapsulating Cy5.5, which has an emission wavelength at 650 nm, which is superior in photon penetration to that of Cy3, were used to monitor the delivery from outside of the body. The time course change of fluorescence intensity from the tumor, which was transplanted into the right femoral region, was monitored as photon counts per second up to 96 h (Fig. 5). An increase in photon counts in tumors was observed from 24 to 96 h after injection with liposomes conjugated to the antibody. The tumor-specific accumulation of liposomes was less significant when the conjugated antibody was less than 3.9 μg/mg lipid. At least 3.9 μg/mg lipid of antibody was required to observe antibody-directed tumor-specific accumulation of liposomes. The increased photon counts in the tumor continued up to 96 h after injection but did not correlate with the amounts of antibody in the range between 3.9 and 7.6 μg antibody/mg lipid. Although a simple passive level of accumulation was also detectable when liposomes without anti-E-selectin antibody were injected, *in vivo* imaging of tumors was only successful when the liposomes were conjugated with anti-E-selectin antibody (Fig. 6).

3. DISCUSSION

Vascular endothelial cells in solid EAT should conceivably be stimulated to express E-selectin *in vivo* as well as *in vitro* (Fig. 2 and 4), resulting in the tumor specific accumulation of liposomes with anti-E-selectin antibody. In our previous study, when liposomes were conjugated with sialyl Lewis^X (SLX), the fluorescence in tumors achieved a maximum at 48 h after injection and then gradually decreased by 96 h after injection (22). In contrast, photon counts of fluorescence from Cy5.5-labeled liposomes in the tumors increased during 72 h and were maintained at a high level up to 96 h after injection when the liposomes were conjugated with anti-E-selectin antibody. The high affinity of liposomes to E-selectin might account for the difference in retention time of fluorescence between the SLX and anti-E-selectin antibody. Monovalent SLX to E-selectin is very weak (K_d, mM) relative to the affinity of antibody to E-selectin (K_d, nM), which results in efficient uptake into tumor tissue (23). Thus longer retention times of liposomes in tumors could be expected when liposomes are conjugated to anti-E-selectin antibody. Considering the fact that pin-point active targeting *in vivo* has been extremely difficult so far (4,5,17), the modification of the liposome surface with a negative charge that was used in this study should also be important. We introduced a negative charge on the surface of liposomes since this modification allowed liposomes that had been conjugated

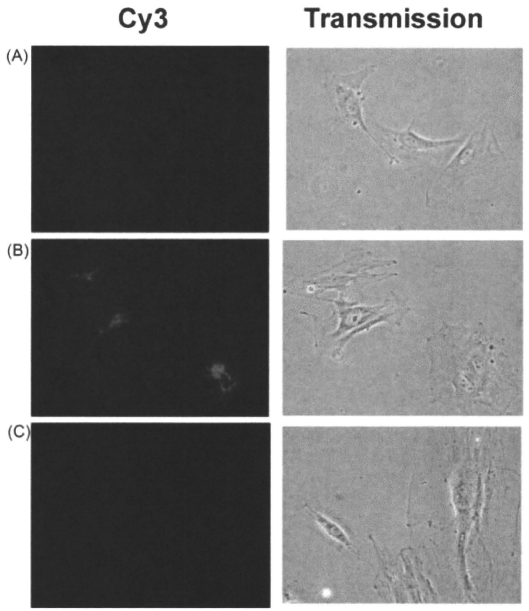

Figure 3. Binding of Cy3-liposomes conjugated with anti-E-selectin antibody to HUVEC. HUVEC was stimulated with TNF-α in advance to express E-selectin. Cy3-liposomes without anti-E-selectin antibody (A) or with anti-E-selectin antibody (3.9 μg/mg lipid) (B) were incubated with HUVEC expressing E-selectin at 37 °C for 30 min, respectively. E-selectin on HUVEC was masked with unlabeled anti-E-selectin antibody by incubation for 30 min prior to the incubation with Cy3-liposomes with anti-E-selectin antibody (3.9 μg/mg lipid) for 30 min (C). Cells were observed under a fluorescence microscope. Magnification was × 40.

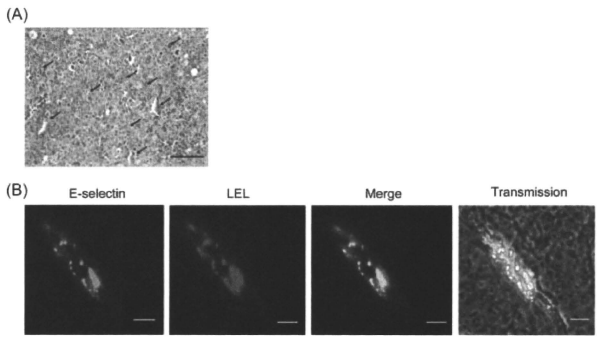

Figure 4. The expression of E-selectin in vascular vessels of solid EAT section. (A) Several vascular vessels (arrows) were observed in HE staining section in one visual field. Scale bar: 100 μm. (B) Double staining of the blood vessel for E-selectin and *Lycopersicon esculentum* lectin (LEL). After deparafinized, the sections were incubated with anti-E-selectin antibody (10 μg/ml) for 1 h at 37 °C, then incubated with goat anti-mouse FITC IgG secondary antibody (green fluoresence) and Texas red conjugated LEL (Red fluoresence) for 1 h at room temperature. Scale bar: 20 μm.

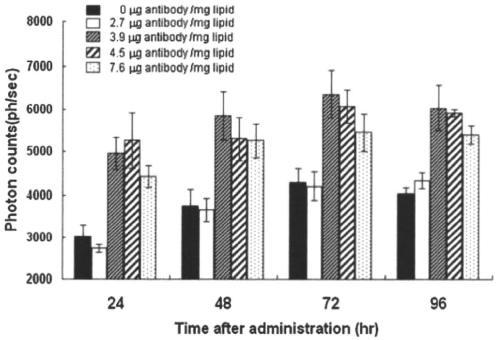

Figure 5. Accumulation of Cy5.5-liposomes conjugated with anti-E-selectin antibody in tumor regions. Cy5.5-liposomes conjugated with anti-E-selectin antibody at 0, 2.7, 3.9, 4.5 and 7.6 μg antibody/mg lipid were injected from the tail veins of EAT tumor-bearing mice. The fluorescence excited at 680 nm was detected as emission spectrum at 700 nm from the tumor region of the same mouse after 24, 48, 72 and 96 h of injection and photons per second were counted. Each vertical bar indicates mean ± SD at $n = 3$.

with antibody to have a long half-life in blood resulting in efficient and active targeting of tumors *in vivo* (24–27). Simultaneously, a hydrophilic surface is established on the liposomes. The repulsive force between the liposomes and the wall of blood vessels should enhance the retention in the vascular system. All of these modifications might assist the liposomes for *in vivo* imaging of tumor by targeting E-selectin and escaping from RES, opsonin proteins in blood plasma and uptake by phagocytotic macrophages. However, *in vivo* imaging from the abdominal side of the animal showed high fluorescence in the liver 72 h after administration (data not shown). As a result, efficient and specific accumulation of liposome-conjugated antibodies could be observed in the final target region with the exception of the liver.

Here we successfully demonstrated visualization of tumors, in which tumor-associated vascular endothelial cells were expressing E-selectin presumably as a consequence of angiogenic factors that were secreted from the tumor, with liposomes conjugated to an anti-E-selectin antibody. Although we did not evaluate an inflammatory model in this report, E-selectin should also be expressed on endothelial cells in inflammatory regions. Recently, nanoparticles conjugated with SLX which were designed for MRI imaging have been reported to image regions of inflammation in the brain for a short time (28). In this context, E-selectin targeting should also be useful for visualization of inflammatory regions *in vivo*. While it is important to distinguish these two different states of tissues, E-selectin targeting should be significantly useful for diagnosis and treatment since inflammation is a well-known risk factor for tumor development and correlates with increased invasiveness and prognosis in a variety of cancers (29). In this report, the maximum accumulation of liposomes conjugated with anti-E-selectin antibody in tumors was achieved 72 h after administration. The accumulation of the liposomes started right after administration and the tumor region could be visualized even 1 h after administration. However, the background was still higher, presumably due to the majority of liposomes circulating in blood vessels.

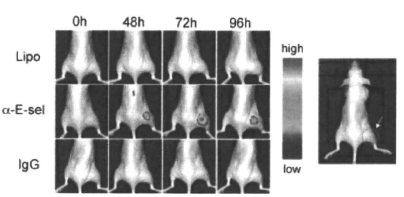

Figure 6. *In vivo* imaging of tumor regions targeting E-selectin. Cy5.5-liposomes without antibody (Lipo), Cy5.5-liposomes conjugated with non-specific porcine antibody at 3.9 μg antibody/mg lipid (IgG) or Cy5.5-liposomes conjugated with anti-E-selectin antibody at 3.9 μg antibody/mg lipid (α-E-sel) were injected into the tail veins of EAT tumor bearing mice. The white arrow indicates tumor region. Images of fluorescence excited at 680 nm were detected as emission spectra at 700 nm in the tumor regions. Each panel was observed at 48, 72 and 96 h after injection.

4. CONCLUSIONS

In this report we have successfully shown that the liposomes conjugated with an anti-E-selectin antibody are available as efficient and specific vectors for imaging *in vivo* targeting to tumor regions. Therefore, the liposomes conjugated with an anti-E-selectin antibody should also be useful as a drug delivery vector of anti-cancer agents. Very recently, lymphatic endothelium has been reported to be sensitive to chemokines for induction of E-selectin *in vitro* (30). The liposomes described in this study might be useful for the identification of sentinel lymphatic nodes. Furthermore, efficient encapsulation of anti-cancer agents into these liposomes should lead to the development of a novel therapeutic technology targeting neovascularization induced by the cytokines secreted from tumors. Since a number of antigens

specific to cancers and other diseases are now being extensively evaluated in various fields, the choice of suitable antibodies specific to these antigens would allow proper delivery of liposomes for therapy. In this context, the present technology should be useful as an active and selective targeting drug delivery system conveying chemical compounds, proteins and nucleic acids, as well as *in vivo* imaging reagents to tumors.

5. EXPERIMENTAL PROCEDURES

5.1. Preparation of anti-E-selectin monoclonal antibody

Female BALB/c mice (6 weeks old) were purchased from Japan SLC. Five hundred micrograms per mouse of pristine (Sigma-Aldrich) was administered twice into the peritoneal cavity of mice with a 5-day interval. At 5 days after the second administration of pristine, 1×10^7 cells of CCL-3 hybridoma (ATCC) producing anti-E-selectin monoclonal antibody were transplanted into the peritoneal cavity. After 20 days, ascites fluid was collected. Ammonium sulfate precipitation was then performed, and the antibody was purified using an affinity purification system (HiTrap Protein G columns, GE Healthcare).

5.2. Preparation of liposomes conjugated with antibody

Preparation of hydrophilic anionic liposomes and encapsulation of Cy3 or Cy5.5 were carried out as described previously (22). The concentration of Cy dye was estimated according to the absorbance at 580 nm for Cy3 and at 680 nm for Cy5.5 measured by Ultrospec 6300 pro (Amersham Biosciences). These liposomes were basically composed of dipalmitoylphosphatidylcholine (DPPC), dipalmitoylphosphatidylethanolamine (DPPE), dicetylphosphate (DCP), cholesterol and ganglioside. DCP was used to confer a negative charge to the liposome surface. Tris(hydroxymethyl)aminomethane (Tris) was crosslinked on the liposome surface via bis(sulfosuccinimidyl)suberate (BS_3; Pierce) to confer hydrophilicity. Using 3,3′-dithiobis(sulfosuccinimidyl)propionate (DTSSP; Pierce), the anti-E-selectin antibody was crosslinked to human serum albumin (HSA; Sigma), which was then coupled in advance to the ganglioside component of liposomes as described previously (22). Anti-E-selectin monoclonal antibody was added to a final concentration of 50, 75, 100, 200 or 300 μg/ml and stirred at 25°C for 2 h. Tris–HCl was then added to reach a final concentration of 132 mg/mL, and stirred overnight at 4°C for hydrophilization of the liposome surface (Fig. 1). As a control, liposomes without antibody and liposomes conjugated with IgG (porcine) were also prepared. IgG was added to a final concentration of 75 μg/ml. The preparation of liposome without antibody was the same as in the case of antibody-liposomes except for the step for binding antibody.

5.3. Measurement of lipid concentration

The content of lipid in liposomes was determined as total cholesterol in the presence of 0.5% TritonX-100 with a Determiner TC555 kit (Kyowa) and the total amount of fatty acids was calculated from the molar ratio of each lipid.

5.4. Measurement of particle size and ζ-potential

The liposome solution was diluted 50 times with distilled water and size distribution and ζ-potentials of liposome particles were measured at 25°C using Zetasizer Nano-S90 (Malvern).

5.5. Quantification of antibody conjugated to the liposome

The amount of anti-E-selectin antibody on the surface of the liposome was measured by enzyme-linked immunosorbent assay (ELISA). Human E-selectin-Fc Chimera (R&D systems) was dissolved in the PBS (pH 7.2) to a final concentration of 2 mg/ml. Fifty microliters of the solution was added to each well of a 96-well plate (Falcon 3072, Falcon) and maintained at 25°C for 1 h for immobilization. After discarding the solution of each well, 300 μl of PBS containing 2% bovine serum albumin (BSA) was added to each well for blocking and incubated at 25°C for 2 h. Each well was then washed three times with PBS. Two milligrams per milliliter of anti-E-selectin antibody was diluted with PBS to a final concentration of 2.4, 1.2, 0.6 or 0.3 μg/ml (standard solution). One hundred microliters of standard solution and liposomes with anti-E-selectin antibody were added to each well of a 96-well plate and incubated at 25°C. After 1 h, the solution of each well was discarded and the well was washed three times with PBS. Next, 100 μl of anti-mouse IgG goat antibody which was labeled with HRP (Santa Cruz Biotechnology) diluted 8000-fold with PBS containing 10% Tween20, and 9% EDTA was added to each well and stood at 25°C for 1 h. After three washes with PBS, 100 μl of TMB Stabilized Substrate for HRP (Promega) was added to each well and reacted at 25°C for 20 min. Each well was then washed three times with PBS and 100 μl of 2 M sulfuric acid was added to each well to stop the reaction. The absorbances of standards and samples were measured at 405 nm using a microplate-reader (BioRad). The binding reactions of antibody were repeated three times and the results were expressed as mean ± SD.

5.6. Detection of E-selectin expressed on HUVEC

Ehrlich ascites tumor cells (CCL-77, ATCC) were cultured in DMEM (Sigma) supplemented with 10% fetal bovine serum (Biowest), 1 mg/ml streptomycin (Sigma) and 100 U/ml penicillin (Sigma) at 37°C in a humidified atmosphere of 5% CO_2 and air. The conditioned medium from EAT cells at 100% confluence was prepared and used as described below. Human umbilical vein endothelial cells (D&S Pharma) were cultured in a medium recommended for HUVEC (Medium for HUVEC, D&S Pharma). To each well of a 12-well plate, 1×10^5 cells of HUVEC in 500 μl medium were added and cultured at 37°C under 5% CO_2. To determine whether E-selectin is induced on the surface of HUVEC by the culture supernatant of the EAT cells, 500 μl of EAT conditioned medium (100% confluent) was added to HUVEC and cultured for 4 h. To induce E-selectin on HUVEC as a positive control, human TNF-α (R&D Systems) was added to a final concentration of 10 ng/ml and HUVEC were cultured for 4 h. As a negative control, 500 μl of DMEM supplement with 1 mg/ml streptomycin, 100 U/ml penicillin and 10% FBS was added to HUVEC and cultured for 4 h. The cells were washed with PBS and fixed with 3.7% formaldehyde for 10 min at 25°C. After washing with PBS containing 0.1% TritonX-100, 500 μl of PBS containing 0.1% BSA was added for blocking to the cells and incubated for 20 min at 25°C. The cells were then incubated in 10 μg/ml of anti-E-selectin monoclonal antibody at 25°C for 1 h. After washing with PBS, FITC labeled anti-mouse IgG antibody (Santa Cruz), which was diluted with 0.1% BSA (final concentration 5 μg/ml), was added and reacted for 1 h at 25°C. To stain for actin filaments, the cells were washed with PBS and incubated in 5 U/ml of rhodamine phalloidin solution (Molecular probes) at 25°C

for 20 min. After washing with PBS and distilled water, HUVEC were analyzed with a fluorescence microscope (CKX41, Olympus).

5.7. E-selectin targeting in vitro

Liposomes encapsulating Cy3 were used through these experiments. Ten microliters of liposomes conjugated with 3.9 μg of anti-E-selectin antibody per milligram of lipid was added to the wells of a 12-well plate containing HUVEC and incubated at 37°C for 30 min under 5% CO_2. After washing three times with PBS, 500 μl of medium was added to each well and incubated for 3 h. Liposomes without antibody were used as negative control. Binding inhibition was carried out to demonstrate that the binding of liposomes to HUVEC was antigen specific. To block the E-selectin on the cells, 100 μg of unlabeled anti-E-selectin monoclonal antibody was added to HUVEC expressing E-selectin. After washing three times with PBS, 500 μl of medium for HUVEC was added. Then, 10 μl of Cy3 encapsulated liposomes with anti-E-selectin antibody (3.9 μg antibody/mg lipid) was added to each well and incubated for 30 min. Each well was then washed three times with PBS and the cells were analyzed using a fluorescence microscope (CKX41, Olympus).

5.8. Detection of E-selectin in vascular vessel of solid EAT section

EAT cells (5×10^6 cells/mouse) were transplanted subcutaneously in the back of female BALB/c nude mice. After 10 days, tumors were excised and fixed in 10% neutral formalin solution (Wako) for 24 h. After fixation, the tissues were dehydrated, cleared, infiltrated and then embedded with paraffin. Then 4 μm thick sections were cut for hematoxylin and eosin staining and for immunohistochemistry. For double staining with fluorescence labeled antibodies, sections were deparafinized and stained as following. After blocking with 10% goat serum containing 3% TritonX-100 for 1 h at room temperature, sections were incubated with anti-E-selectin antibody (10 μg/ml) for 1 h at 37°C and then rinsed three times in PBS for 5 min each. Sections were further incubated with goat anti-mouse FITC labeled IgG antibody (Santa Cruz) diluting 200 times and Texas red conjugated *Lycopersicon esculentum* (tomato) lectin (Vector) diluting 100 times for 1 h at room temperature in dark and then rinsed three times in PBS for 5 min each in dark. The sections were mounted with glycerol-PBS (9:1) and then observed with an Olympus IX81 microscope equipped with a reflected light fluorescence device (Olympus).

5.9. E-selectin targeting in vivo

Liposomes encapsulating Cy5.5 were used throughout this experiment. EAT cells (5×10^6 cells/mouse) were transplanted subcutaneously to the right femoral region or to the right side in the back of female BALB/c mice (6 weeks old), and used for experiments 10 days later. To optimize the amount of antibody, 200 μl of liposomes conjugated with various amount of anti-E-selectin antibody was injected via the tail vein. Then photon count per second of Cy5.5 in the tumor at the right femoral region of the same mouse was measured with eXplore Optix (excitation at 680 nm and emission at 700 nm; GE Healthcare), under isoflurane anesthesia before and after injection. Three mice were used in each experimental group. The results of photon counts per second are expressed as mean ± SD. For *in vivo* imaging, 200 μl of liposomes conjugated with 3.9 μg of anti-E-selectin antibody/mg lipid was injected from the tail vein. Simultaneously, 200 μl of liposomes conjugated with normal porcine IgG (Sigma) and liposomes without antibody were injected as control. The signal of Cy5.5 in the tumor transplanted at the right side in back of mouse was monitored under isoflurane anesthesia with IVIS Lumina-II (excitation at 680 nm and emission at 700 nm; Caliper Life Sciences).

All animal experiments through this study were conducted in full compliance with local, national, ethical and regulatory principles for animal care.

Acknowledgements

We thank Dr David S. Salomon (NCI, Bethesda, MD, USA) for reading this manuscript and for enthusiastic discussions and suggestions.

REFERENCES

1. Frangioni JV. In vivo near-infrared fluorescence imaging. Curr Opin Chem Biol 2003; 7: 626–634.
2. Maruyama K, Yuda T, Okamoto A, Kojima S, Suginaka A, Iwatsuru M. Prolonged circulation time *in vivo* of large unilamellar liposomes composed of distearoyl phosphatidylcholine and cholesterol containing amphipathic poly (ethylene glycol). Biochim Biophys Acta 1992; 1128: 44–49.
3. Gabizon A, Papahadjopoulos D. Liposome formulation with prolonged circulation time in blood and enhanced uptake by tumors. PNAS 1988; 85: 6949–6953.
4. Vyas SP, Singh A, Sihorkar V. Ligand-receptor-mediated drug delivery: an emerging paradigm in cellular drug targeting. Crit Rev Ther Drug Carrier Syst 2001; 18: 1–76.
5. Willis M, Forssen E. Ligand-targeted liposomes. Adv Drug Deliv Rev 1998; 29: 249–271.
6. Kessner S, Krause A, Rothe U, Bendas G. Investigation of the cellular uptake of E-selectin-targeted immunoliposomes by activated human endothelial cells. Biochim Biophys Acta 2001; 1514: 177–190.
7. Klivanov AL, Maruyama K, Beckerleg AM, Torchilin VP, Huang L. Activity of amphipathic poly (ethylene glycol) 5000 to prolong the circulation time of liposomes depends on the liposome size and is unfavorable for immunoliposomes binding to target. Biochim Biophys Acta 1991; 1062: 142–148.
8. Bevilacqua MP, Stengelin S, Gimbrone MA, Seed B. Endothelial leukocyte adhesion molecule 1: an inducible receptor for neutrophils related to complement regulatory proteins and lectins. Science 1985; 243: 1160–1165.
9. Vestweber D, Blanks JE. Mechanisms that regulate the function of the selectins and their ligands. Physiol Rev 1999; 79: 181–213.
10. Mayer B. De novo expression of the cell adhesion molecule E-selectin on gastric cancer endothelium. Langenbeck's Arch Surg 1998; 383: 81–86.
11. Liu F, Rabinovich GA. Galectins as modulators tumor progression. Nature Rev Cancer 2005; 5: 29–41.
12. Pober JS, Bevilacqua MP, Mendrick DL, Lapierre LA, Fiers W, Gimbrone MA. Two distinct monokines, interleukin 1 and tumor necrosis factor, each idependently induce biosynthesis and transient expression of the same antigen on the surface of cultured human vascular endothelial cells. J Immunol 1986; 136: 1680–1687.
13. Kim I, Moon SO, Kim SH, Kim HJ, Koh YS, Koh GY. Vascular endothelial growth factor expression of intercellular adhesion molecule 1 (ICAM-1), vascular cell adhesion molecule 1 (VCAM-1), and E-selectin through nuclear factor-kappa B activation in endothelial cells. J Biol Chem 2001; 276: 7614–7620.
14. Ehrhardt C, Kneuer C, Bakowsky U. Selectin – an emerging target for drug delivery. Adv. Drug Deliv 2004; 56: 527–549.
15. Dodd RB, Drickamer K. Lectin-like proteins in model organisms: implications for evolution of carbohydrate-binding activity. Glycobiology 2001; 11: 71R–79R.
16. Kilpatrick DC. Animal lectins: a historical introduction and overview. Biochim Biophys Acta 2002; 1572: 187–197.

17. Spragg DD, Alford DR, Greferath R, Larsen CE, Lee KD, Gurtner GC, Cybulsky MI, Tosi PF, Nicolau C. Immunotargeting of liposomes to activated vascular endothelial cells; A strategy for site-selective delivery in the cardiovascular systems. Proc Natl Acad Sci USA 1997; 94: 8795–8800.
18. Stahn R, Grittner C, Zeisig R, Karsten U, Felix SB, Wenzel K. Sialyl Lewis (X)–liposomes as vehicles for site-directed, E-selectin-mediated drug transfer into activated endothelial cells. Cell Mol Life Sci 2001; 58: 141–147.
19. Tan PH, Manunta M, Ardjomand N, Xue SA, Larkin DF, Haskard DO, Taylor KM, George AJ. Antibody targeted gene transfer to endothelium. J Gene Med 2003; 5: 311–323.
20. Zeising R, Stahn R, Wenzel K, Behrens D, Fichtner I. Effect of sialyl LewisX-glycoliposomes on the inhibition of E-selectin-mediated tumor cell adhesion *in vitro*. Biochim Biophys Acta 2004; 1660: 31–40.
21. Murphy TJ, Thurston G, Ezaki T, McDonald DM. Endothelial cell heterogeneity in venules of mouse airways induced by polarized inflammatory stimulus. Am J Pathol 1999; 155: 93–103.
22. Hirai M, Minematsu H, Kondo N, Oie K, Igarashi K, Yamazaki N. Accumulation of liposome with Sialyl Lewis X to inflammation and tumor region: application to *in vivo* bio-imaging. Biochem Biophys Res Commun 2007; 353: 553–558.
23. Thomas VH, Yang Y, Rice KG. In vivo ligand specificity of E-selectin binding to multivalent sialyl LewisX N-Linked oligosaccharides. J Biol Chem 1999; 274: 19035–19040.
24. Yamazaki N, Kojima S, Yokoyama H. Biomedical nanotechnology for active drug delivery systems by applying sugar-chain molecular functions. Curr Appl Phys 2005; 5: 112–117.
25. Yamazaki N. Analysis of the carbohydrate-binding specificity of lectin-conjugated lipid vesicles which interact with polysaccharide fragment. J Membr Sci 1989; 41: 249–267.
26. Yamazaki N, Kodama M, Gabius H-J. Neoglycoprotein–liposome and lectin–liposome conjugates as tools for carbohydrate recognition research. Meth Enzymol 1994; 242: 56–65.
27. Hashida N, Ohguro N, Yamazaki N, Arakawa Y, Oiki E, Mashimo H, Kurikawa N, Tano Y. High-efficacy site-directed drug delivery system using Sialyl–Lewis X conjugate liposome. Exp Eye Res 2008; 86: 138–149.
28. Van Kasteren SI, Campbell SJ, Serres S, Anthony DC, et al. Glyconanoparticles allow pre-symptomatic *in vivo* imaging of brain disease. Proc Natl Acad Sci 2009; 106: 18–23.
29. Coussens LM, Web Z. Inflammation and cancer. Nature 2002; 420: 860–867.
30. Sawa Y, Tsuruga E. The expression of E-selectin and chemokines in the cultured human lymphatic endothelium with lipopolysaccharides. J Anat 2008; 212: 654–663.

International Journal of Pharmaceutics 391 (2010) 274–283

Contents lists available at ScienceDirect

International Journal of Pharmaceutics

journal homepage: www.elsevier.com/locate/ijpharm

Pharmaceutical Nanotechnology

Novel and simple loading procedure of cisplatin into liposomes and targeting tumor endothelial cells

M. Hirai[a,b], H. Minematsu[a], Y. Hiramatsu[a], H. Kitagawa[a], T. Otani[a,b], S. Iwashita[a], T. Kudoh[b], L. Chen[b], Y. Li[b], M. Okada[b], D.S. Salomon[c], K. Igarashi[a], M. Chikuma[d], M. Seno[b,*]

[a] R&D Division, Katayama Chemical Industries Co., LTD, Minoh, Osaka 562-0015, Japan
[b] Department of Medical and Bioengineering Science, Graduate School of Natural Science and Technology, Okayama University, Okayama 700-8530, Japan
[c] Tumor Growth Factor Section, Mammary Biology and Tumorigenesis Laboratory, Center for Cancer Research, National Cancer Institute, Bethesda, MD 20892, USA
[d] Osaka University of Pharmaceutical Sciences, Takatsuki, Osaka 569-109, Japan

ARTICLE INFO

Article history:
Received 20 August 2009
Received in revised form 1 January 2010
Accepted 27 February 2010
Available online 6 March 2010

Keywords:
Cisplatin
Cis-diamminedinitratoplatinum (II)
Liposome
E-selectin
Sialyl Lewis^X

ABSTRACT

Although intravenous administration of high levels of cisplatin (CDDP) are limited due to its severe side effects, efficient delivery of CDDP directly to the tumor should improve the therapeutic response while potentially by-passing significant side effects.

High loading of CDDP into liposomes is one technique that could be used as a potential drug delivery system. Since *cis*-diamminedinitratoplatinum (CDDP3) is highly soluble in water and converts to CDDP in the presence of chloride ions, we encapsulated CDDP3 into liposomes in the absence of chloride ions and supplemented chloride ions to prepare CDDP-encapsulated liposomes (CDDP-Lip) resulting in a significantly improved loading efficiency of CDDP. We further conjugated the CDDP-Lip with Sialyl Lewis^X (CDDP-SLX-Lip) because we previously demonstrated Sialyl Lewis^X enhanced efficient accumulation of liposomes into tumors in vivo. CDDP-SLX-Lip treated mice showed a survival rate of 75% at 14 days even if a lethal level of CDDP was injected into mice. Loss of body weight was negligible and no histological abnormality was found in a variety of normal tissues. Accumulation of CDDP-SLX-Lip was about 6 times more than that of CDDP-Lip or CDDP. As the result, there was better antitumor activity of CDDP-SLX-Lip than that of CDDP-Lip with significantly less toxic effects in normal tissues.

1. Introduction

Cisplatin (*cis*-diamminedichloroplatinum, CDDP) is one of the most widely used chemotherapeutic drugs in the clinical treatment of a variety of tumors, such as lung, ovarian and gastric carcinomas (Comis, 1994). However, administration of escalating doses of CDDP is limited because of severe side effects such as nephrotoxicity, hematopoietic injury, and deafness (Cvitkovic et al., 1977; Hayes et al., 1977; Von Hoff et al., 1979; Goldstein et al., 1981). Efforts to decrease these deleterious side effects by screening various CDDP derivatives and by developing improved forms of dosage or methods of medication have been unsuccessful (Borch and Markman, 1989; Ogilvie et al., 1992; Legha et al., 1992; Navari et al., 1994). Practical drug delivery systems, which specifically recognize tumors to efficiently deliver drugs at high doses *in vivo*, have also been undertaken. However, as yet no efficient carriers to efficiently deliver CDDP to tumors have been developed (Bandak et al., 1999; Newman et al., 1999; Vaage et al., 1999). Among the several liposomal formulations of CDDP, the latest is SPI-077, in which CDDP is encapsulated in pegylated stealth liposomes (Newman et al., 1999). Although preclinical studies showed that compared with the free drug, SPI-077 exhibited improved stability, prolonged circulation time, increased antitumor effect, and reduced side effects (Newman et al., 1999; Vaage et al., 1999), little antitumor activity of SPI-077 was observed in Phase I/II studies (Harrington et al., 2001; Kim et al., 2001; Veal et al., 2001). The major problem of conventional liposomal formulations involving CDDP, such as in SPI-077, was the extremely low drug to lipid weight ratio due to water insolubility and low lipophilicity of CDDP, which resulted in failure to adequately deliver the drug to the tumor (Bandak et al., 1999; Meerum Terwogt et al., 2002).

In contrast with CDDP, *cis*-diamminedinitratoplatinum (II) (CDDP3), one of the various CDDP derivatives, is highly water soluble and is readily converted into CDDP in the presence of chloride

Abbreviations: SLX, Sialyl Lewis^X; CDDP, *cis*-diamminedichloroplatinum (II) or cisplatin; CDDP3, *cis*-diamminedinitratoplatinum (II); SLX-Lip, liposomes modified with SLX; CDDP-Lip, liposomes containing CDDP; CDDP-SLX-Lip, liposomes modified with SLX containing CDDP; LEL, *lycopersicon esculentum* lectin.

* Corresponding author at: Room 361, Bldg. ENG-6, Laboratory of Nano-Biotechnology, Department of Medical and Bioengineering Science, Graduate School of Natural Science and Technology, Okayama University, 3.1.1 Tsushima-Naka, Kita-ku, Okayama 700-8530, Japan. Tel.: +81 86 251 8216; fax: +81 86 251 8216.
E-mail address: mseno@cc.okayama-u.ac.jp (M. Seno).

0378-5173/$ – see front matter © 2010 Elsevier B.V. All rights reserved.
doi:10.1016/j.ijpharm.2010.02.030

ions (Dhara, 1970). In this study we exploited this character of CDDP3, to establish an efficient procedure of CDDP encapsulation into liposomes at a high concentration.

As for the precedent targeting delivery of CDDP, cationic liposomes conjugated with 3,5-dipentadecycloxybenzamidine hydrochloride (TRX-20) encapsulating CDDP were shown to be significantly effective to suppress tumor growth and liver metastasis targeting chondroitin sulfate proteoglycans on the malignant cell surface (Lee et al., 2002). Here in this study, we employed a new formula for anionic liposomes conjugated with Sialyl Lewis^X (SLX), which specifically and efficiently targeted E-selectin and accumulated in tumors *in vivo* (Hirai et al., 2007a,b). Liposomes with SLX showed affinity to E-selectin expressed on tumor vascular endothelial cells and exhibited rolling action on the vascular endothelial cells. The SLX-coated liposomes then entered the gaps of the vascular walls, where permeability is augmented by tumor angiogenesis (Bevilacqua et al., 1989; Vestweber and Blanks, 1999; Mayer et al., 1998; Liu and Rabinovich, 2005).

2. Materials and methods

2.1. Materials

CDDP, potassium tetrachloroplatinate (II), potassium iodide, ammonia aqueous solution (28%), silver nitrate, dipalmitoylphosphatidyl choline (DPPC), cholesterol (Chol), dicetylphosphate (DCP), sodium cholatehydrate (cholic acid) human serum albumin (HSA), sodium periodate, deuterium oxide (D_2O) sodium hexachloroplatinate, tris(hydroxymethyl)aminomethane (Tris), DMEM, RPMI-1640, gelatin, fetal bovine serum (FBS) and penicillin–streptomycin solution were purchased from Sigma (St. Louis, MO). Ganglioside was purchased from Avanti Polar Lipids (Alabaster, AL, USA). Dipalmitoylphosphatidylethanolamine (DPPE) was purchased from Alexis (Plymouth Meeting, PA). N-tris(hydroxymethyl)methyl-3-amino-propane sulfonic acid (TAPS) and *n*-(2-hydroxyethyl) piperazine-*n*′-(2-ethanesulfonic) acid were purchased from Dojin Chemical (Kumamoto, Japan). Sodium cyanoborohydrate was purchased from Aldrich (Milwaukee, WI). Sialyl Lewis^X (SLX) was purchased from EMD Chemicals (Gibbstown, NJ). Bis(sulfosuccinimidyl)suberate (BS_3) and 3,3-dithiobis(sulfosuccinimidylpropionate) (DTSSP) were purchased from Pierce Biotechnology (Rockford, IL, USA). Determiner TC555 kit was purchased from Kyowa Medics (Tokyo, Japan). Potassium dichloroplatinum was purchased from Nacalai Tesque (Kyoto, Japan). In situ apoptosis detection kit was purchased from Takara BIO (Kyoto, Japan). TNF-α was purchased from R&D Systems (Minneapolis, MN). FITC labeled anti-mouse IgG antibody was purchased from Santa Cruz (Santa Cruz, CA). Collagen was purchased from Roche (Basel, Switzerland). Female BALB/c mice were purchased from Japan SLC (Shizuoka, Japan). Ehrlich's ascites tumor (EAT) cells were purchased from RIKEN Bio Resource Center (Ibaragi, Japan). Human lung cancer A549 cells and Hybridoma (CCL-3) were obtained from the ATCC (Manassas, VA). Human umbilical vein endothelial cells (HUVEC) and human endothelial cell medium were purchased from DS Pharma Biomedical (Osaka, Japan).

2.2. Preparation of CDDP3

CDDP3 was synthesized by the method of Dhara (1970). Briefly, potassium tetrachloroplatinate (II) (4.15 g, 10 mmol) was dissolved in distilled water. Potassium iodide (6.64 g, 40 mmol) was then added and stirred on ice for 5 min under a nitrogen atmosphere and light shielding. Ammonia aqueous solution (28%, 1.35 mL) was added to this reaction solution, and stirred on ice for 3 h. The yellow crystals formed were washed with distilled water and ethanol, and dried at 40 °C for 10 h under decompression. At this stage, 4.49 g of *cis*-diammindiiodeplatinum (II) (CDDP2) was obtained. CDDP2 (2.41 g, 5 mmol) was suspended in distilled water. Silver nitrate (1.68 g, 9.9 mmol) was then added and stirred on ice for 24 h under light shielding. The reaction solution was passed through a paper filter to remove any silver iodide. The filtrate was then concentrated using a rotating evaporator and white crystals were obtained. These crystals were washed with iced distilled water and ethanol, and then dried at 40 °C for 10 h under decompression. The final yield of CDDP3 was 1.0 g.

2.3. Measurement of absorption spectrum

The absorption spectra were measured using a UV spectrophotometer (Model UV-2500PC, Shimazu, Japan) at 5, 10, 15, 30, 60, 120 and 180 min after dissolving 5 mg of CDDP3 in 1 mL of 150 mM NaCl. In contrast, 2 mg of CDDP was dissolved in 1 mL of 150 mM NaCl and 24 h after dissolution, the absorption spectrum was measured. The absorption spectrum of 150 mM NaCl was deducted from each absorption spectrum.

2.4. Preparation of CDDP-encapsulated liposomes

The liposomes were prepared using an improved cholate dialysis method (Yamazaki, 1989; Yamazaki et al., 1994). DPPC, Chol, ganglioside, DCP and DPPE were mixed at the molar ratio 35:40:5:15:5 (total lipid 456 mg) and then cholic acid (469 mg) was added to facilitate micelle formation. The mixture was dissolved in 30 mL of methanol/chloroform (1:1, v/v) solution. The solvent was evaporated using a rotating evaporator at 37 °C to produce a lipid film, which was dried under vacuum. This lipid film was dissolved in 30 mL of 10 mM TAPS buffer without NaCl at pH 8.4, followed by sonication to obtain a suspension of uniform micelles. One gram of CDDP3 was completely dissolved in 70 mL of 10 mM TAPS (pH 8.4), without NaCl and the pH was readjusted to 8.4 with 1 M NaOH. The CDDP3 solution was then added to the micelle suspension described above. To subsequently remove cholic acid and free CDDP3, the micelle solution was ultrafiltrated with 10 mM TAPS (pH 8.4) using an ultrafiltration cell holder (Amicon model 8200, Millipore, Billerica, MA) fitted with an ultrafiltration disc membrane (molecular cut off 10,000) (Amicon PM10, Millipore, Billerica, MA). One hundred milliliter of the liposome encapsulated CDDP3 was obtained. To convert CDDP3 in the liposomes into CDDP, the buffer was exchanged to 10 mM TAPS, pH 8.4, containing 150 mM NaCl by ultrafiltration through an ultrafiltration disc membrane (molecular cut off: 300,000) (Amicon XM300, Millipore, Billerica, MA). Hydrophilization treatment and SLX conjugation on the surface of liposomes were carried out as described previously (Hirai et al., 2007a). To exchange buffer, the solution was ultrafiltrated with sodium 5 mM hydrogencarbonate buffer (CBS, pH 8.5) through Amicon XM300 membrane. One hundred milligram of the crosslinking agent BS_3 was added to 100 mL of the liposome solution, and stirred at 25 °C for 2 h. The suspension was then further stirred overnight at 4 °C after which BS_3 was conjugated to the liposome surface. Four hundred milligram of Tris was then added, and stirred at 25 °C for 2 h and further stirred overnight at 4 °C to bind Tris to BS_3. The suspension was ultrafiltrated with 10 mM TAPS (pH 8.4) through an Amicon XM300 membrane to remove any residual Tris. Human serum albumin (HSA) was coupled to the liposome surface as previously described (Yamazaki, 1989; Yamazaki et al., 1994). To oxidize the liposome surface, 108 mg of sodium periodate was added to 100 mL of the liposome solution and stirred at 4 °C overnight. To remove residual sodium periodate, the suspension was ultrafiltrated with 10 mM phosphate saline buffer (PBS, pH 8.0) through an Amicon XM300 membrane. Two hundred mil-

ligram of HSA was then added to the suspension and stirred at 25 °C for 2 h. Then 31.3 mg of sodium cyanoborohydrate was added, and stirred at 25 °C for 2 h and further overnight at 4 °C. To remove any residual sodium cyanoborohydrate, the solution was ultrafiltered with CBS buffer (pH 8.5) through an Amicon XM300 membrane. SLX was conjugated to the liposome surface through DTSSP. One hundred milligram of DTSSP, a crosslinking agent, was added to 100 mL of liposomes solution, and stirred at 25 °C for 2 h, and further overnight at 4 °C. To remove residual DTSSP, the solution was ultrafiltrated with CBS buffer (pH 8.5) through an Amicon XM300 membrane. The amination of the reducing group terminal of SLX was accomplished through the glycosyl amination reaction. Eight milligram of SLX was dissolved in 2 mL of distilled water. One gram of ammonium hydrogencarbonate was added and stirred at 37 °C for 3 days. Aminated SLX was added to reach a final concentration of 50 μg/mL and stirred at 25 °C for 2 h. Tris was then added to a final concentration of 132 mg/mL, and stirred overnight at 4 °C for repeated hydrophilization of the liposome surface. To remove any residual SLX and Tris, the solution was ultrafiltrated with 20 mM HEPES (pH 7.2) through an Amicon XM300 membrane. The preparation of liposomes without SLX was similar to the CDDP-SLX-Lip case except for the process for binding SLX. In the studies using animals, CDDP-Lip and CDDP-SLX-Lip were further concentrated 20-fold by ultrafiltration with 20 mM HEPES buffer (pH 7.2) using an Amicon XM300 membrane.

2.5. Physiochemical characterization of CDDP-SLX-Lip

Average particle size and zeta-potential of liposomes that were prepared in water were determined by dynamic light scattering spectrophotometry (Zetasizer Nano-S90, Malvern, Worcestershire, UK) at 25 °C. The instrument was calibrated with standard latex nanoparticles (Malvern, Worcestershire, UK). Experimental values were the average of three different formulations.

2.6. Analysis of lipid concentration

Lipid concentrations of CDDP-Lip and CDDP-SLX-Lip were measured as total cholesterol in the presence of 0.5% TritonX-100 using a Determiner TC555 kit. The lipid concentration was calculated from the molar ratio of each lipid (4.5) by the following formula (Eq. (1)):

$$\text{lipid concentration (mg/mL)} = \text{cholesterol concentration (mg/mL)} \times 4.5 \quad (1)$$

2.7. Measurement of CDDP, calculation of CDDP concentration and definition of encapsulation efficiency and loading efficiency

CDDP-SLX-Lip were diluted to 10,000-fold with distilled water and the concentration of platinum was measured using automatic a flameless atomic absorption spectrophotometer (FAAS) (Model AA-6700, Shimadzu, Kyoto, Japan). Potassium dichloroplatinate was used as a standard. A calibration curve with platinum concentrations in the range of 50–250 ng/mL was run before analysis of each sample type. The amounts of CDDP were calculated by the following formula (Eq. (2)):

$$\text{CDDP concentration} = A \times \frac{300}{195} \quad (2)$$

where A is the concentration of platinum, 300 is the molecular weight of CDDP, and 195 is the molecular weight of platinum. "Encapsulation efficiency" and "loading efficiency" were defined by the following formula Eqs. (3) and (4), respectively.

$$\text{encapsulation efficiency (\%)} = \frac{\text{amount of CDDP in liposomes}}{\text{initial amount of CDDP}} \times 100 \quad (3)$$

$$\text{loading efficiency} = \frac{\text{CDDP concentration (mg/mL)}}{\text{lipid concentration (mg/mL)}} \quad (4)$$

Namely, "CDDP to lipid weight ratio" was defined as "CDDP loading efficiency".

2.8. ^{195}Pt NMR analysis

CDDP-SLX-Lip were concentrated by ultrafiltration using an Amicon XM300 membrane, and suspended in D_2O to a final platinum concentration of 137 mM. CDDP and CDDP3 were dissolved in D_2O to final concentrations of 6.6 and 137 mM, respectively. Sodium hexachloroplatinate was dissolved in D_2O to a final concentration of 50 mM as the external standard liquid. Each sample was put into 5-mm-width NMR sample tubes (GL Sciences, Tokyo, Japan) and ^{195}Pt NMR spectra were measured at 25 °C using NMR system (Model INOVA-600, Varian, Palo Alto, CA, USA).

2.9. Evaluation of CDDP leakage from CDDP-SLX-Lip

CDDP-SLX-Lip were stored in 20 mM HEPES buffer (pH 7.2) at 4 °C for 3 months. To remove any CDDP leakage from CDDP-SLX-Lip, the liposomes solution was ultrafiltrated using an Amicon XM300 membrane. The concentration of platinum incorporated into the liposomes was measured by FAAS and the amount of CDDP was calculated as described above. The CDDP concentration in CDDP-SLX-Lip after storage for 3 months was compared with that of CDDP in the liposomes immediately after preparation.

2.10. Acute toxicity evaluation

CDDP (18 and 25 mg CDDP/kg body weight), CDDP-SLX-Lip (18, 25 and 50 mg CDDP/kg body weight), saline solution and empty liposomes with SLX (lipid: 700 mg/kg body weight) were administered into the tail veins ($n = 4$) of female BALB/c mice (8 weeks) and the survival rate was examined for 14 days after administration. The lipid dose of empty liposomes with SLX was adjusted to the lipid dose in the case of CDDP-SLX-Lip at 50 mg CDDP/kg body weight. The body weight was measured simultaneously as an indicator of systemic toxicity. Body weight was measured for 5 days after administration with electric balance (Model EK-600i, A &D, Tokyo, Japan). Body weight (%) was calculated by the following formula Eq. (5).

$$\text{body weight (\%)} = \frac{\text{body weight at measurement day after injection}}{\text{body weight before injection}} \times 100 \quad (5)$$

The statistical analysis of the body weight change data were carried out by Mann–Whitney U-test.

For histological and histochemical analysis, CDDP or CDDP-SLX-Lip were injected into the tail vein of normal mice with a dose of either 25 mg CDDP/kg body weight. The kidney, spleen and liver were excised at 3 days after administration and fixed in 10% neutral formalin solution. Paraffin-embedded 2 μm-thick sections were stained with hematoxylin and eosin (HE). TUNEL staining was carried out to detect apoptosis with an in situ apoptosis detection kit followed by HE staining.

All the animal experiments throughout this study were conducted in full compliance with local and national ethical and regulatory principles for animal care.

2.11. Cell cultures

EAT cells and A549 cells were cultured in DMEM supplemented with 10% heat-inactivated FBS, 100 U/mL penicillin and 100 μg/mL streptomycin at 37 °C under atmosphere of 5% CO_2/95% air. HUVEC was cultured in medium for HUVEC (KJB-110, DS Pharma, Japan) supplemented with 10% FBS, 100 U/mL penicillin and 100 μg/mL streptomycin at 37 °C under atmosphere of 5% CO_2/95% air.

2.12. Detection of E-selectin on HUVEC

Anti-E-selectin monoclonal antibody was prepared from the ascites fluid of female Balb/c mice (8 weeks), which received CCL-3 hybridoma. Glass slides in 12-well plates were seeded with 1×10^5 HUVEC per well and cells were incubated in 500 μL of medium at 37 °C for 24 h. EAT cells were cultured until 100% confluent. Five hundred microliter of the supernatant culture medium of EAT or the complete medium of EAT was added to 500 μL of the culture medium of HUVEC. TNF-α was added at 10 ng/mL and HUVEC were cultured for 4 h at 37 °C under atmosphere of 5% CO_2/95% air. After 4 h, HUVEC were then fixed with 3.7% formaldehyde in PBS and at room temperature for 15 min and washed twice with PBS and 0.1% TritoX-100 in PBS. 0.1% of BSA in PBS was added to the each well and incubated at room temperature for 20 min. Anti-E-selectin monoclonal antibody was added at 10 μg/mL and incubated at room temperature for 1 h. HUVEC were then washed twice with PBS, stained with 5 μg/mL FITC labeled anti-mouse polyclonal antibody at room temperature for 1 h and washed twice with PBS. For staining cytoskeleton, rhodamine phalloidin was added at 5 U/mL to HUVEC cultures and incubated at room temperature for 20 min and washed twice with PBS and water. The fluorescence of FITC and rhodamine was observed with fluorescent microscope (Model CKX41, Olympus, Tokyo, Japan).

2.13. Detection of E-selectin in vascular vessels of EAT tumor section

EAT cells (5×10^6 cells/mouse) were transplanted subcutaneously in the back of female BALB/C nude mice. After 10 days, tumors were excised and fixed in 10% neutral formalin solution (Wako) for 24 h. After fixation, the tissues were dehydrated, cleared, infiltrated and embedded with paraffin. Then 4 μm-thick sections were cut out for hematoxylin and eosin (HE) staining and for double immunohistochemistry. For immunological staining, sections were deparaffinized and blocked with 10% goat serum containing 3% TritonX-100 for 1 h at room temperature, sections were incubated with anti-E-selectin antibody (10 μg/mL) for 1 h at 37 °C and rinsed three times in PBS for 5 min each. Then sections were further incubated with FITC labeled goat anti-mouse IgG antibody (Santa Cruz) and *lycopersicon esculentum* lectin (LEL) conjugated with Texas red (Vector Labs) for 1 h at room temperature followed by three times of wash with PBS for 5 min. The sections were mounted with glycerol–PBS (9:1) and observed under an Olympus IX81 microscope equipped with a light fluorescence device (Olympus).

2.14. Targeting tumor of CDDP-SLX-Lip

To prepare EAT tumor-bearing mice, 5×10^6 cells were subcutaneously injected into the right femoral region of 6-week-old female BALB/c mice. Ten days after injection, CDDP-SLX-Lip, CDDP-Lip or CDDP were injected into the tail veins at a dose of 2 mg CDDP/kg body weight. At 48 h after administration, the tumors were excised and soaked in 1 mL of 70% HNO_3 per 0.1 g of each tumor tissue followed by incubation in a water-bath at 60 °C for 1 h. After being cooled to room temperature, supernatant was diluted 4-fold with distilled water. To determine the recovery of platinum, blank tumor tissues samples were spiked with 125 ng CDDP for 1 h, followed by digestion with nitric acid and dilution with distilled water. The amount of platinum in the tumor tissues was measured by FAAS and the amounts of CDDP were calculated as described above. The recovery of platinum after incubation of tumor tissues with CDDP was 82–95%. The statistical analysis was carried out by the standard Student's *t*-test.

2.15. In vivo antitumor activity

To prepare A549 tumor-bearing mice, 1×10^7 cells were subcutaneously injected into the right femoral region of 6-week-old female BALB/c mice at 5, 12 and 19 days after injection, CDDP-SLX-Lip, CDDP-Lip or CDDP were injected into the tail veins at a dose of 25 mg CDDP/kg body weight ($n = 4$). Saline solution was injected into control group ($n = 4$). At 5, 12, 19 and 26 days after injection, the length and width of the tumors were measured using digital calipers (Model CD-20C, Mitsutoyo, Japan), and tumor volume was calculated by the following formula (Eq. (6)).

$$\text{volume } (\text{mm}^3) = \text{length} \times \text{width}^2 \times 0.5 \quad (6)$$

The statistical analysis was carried out by the standard Student's *t*-test.

3. Results

3.1. Conversion of CDDP3 to CDDP

CDDP has a structure coordinating chloride ions at the *cis* location (Fig. 1A) while CDDP3 has nitrate ions in place of chloride (Fig. 1B) with solubility in water about 10 times higher than that of

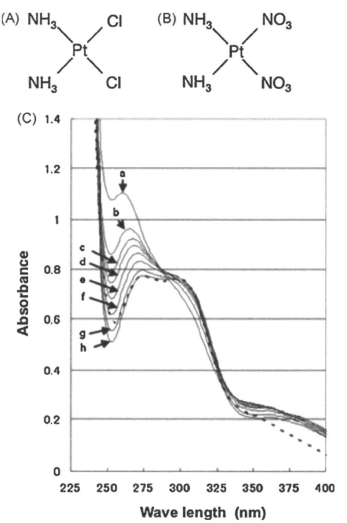

Fig. 1. Conversion from *cis*-diamminedinitratoplatinum (II) (CDDP3) to CDDP. Chemical structures of CDDP (A) and CDDP3 (B). (C) Time-dependent shifts in absorption spectrum of 13.7 mM CDDP3 placed in 150 mM NaCl solution for a, 0; b, 5; c, 10; d, 15; e, 30; f, 60; g, 120; h, 180 min. The dotted line shows the absorption spectrum of 6.6 mM CDDP solution at 24 h after dissolving in 150 mM NaCl solution.

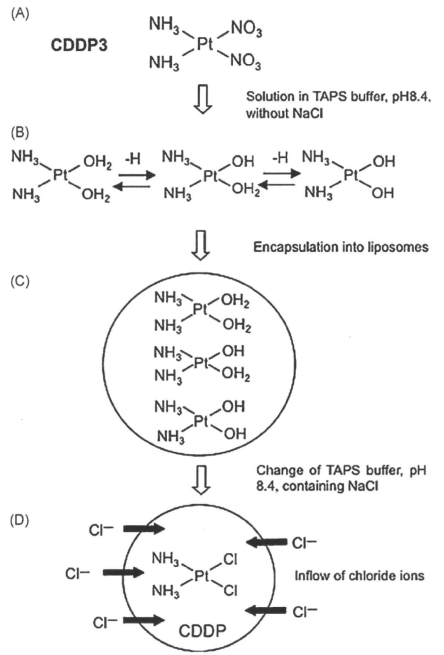

Fig. 2. Scheme of CDDP encapsulation into liposomes using CDDP3. (A) CDDP3 in TAPS, pH 8.4, without NaCl. (B) CDDP3 is in a reversible equilibrium state where H_2O molecules are coordinated due to high solubility of CDDP3 in water. (C) CDDP3 are incorporated in liposomes at this stage, they will show various molecular forms in the liposomes. (D) Change of buffer TAPS, pH 8.4, containing 150 mM NaCl, makes flow of chloride ions into the liposomes and then CDDP is produced by forming coordinate bonds preferentially with chloride ions.

CDDP. The absorption spectra showed that CDDP3 gradually converted to CDDP during incubation in 150 mM NaCl for 24 h (Fig. 1C). Since CDDP3 is soluble in water and stable under chloride ion free conditions, encapsulation of CDDP3 into liposomes at high concentrations as depicted in Fig. 2 should be feasible since the low solubility of CDDP in water impairs encapsulation into liposomes. CDDP3 was encapsulated into liposomes with SLX and the conversion to CDDP in the presence of chloride ions was monitored as the chemical shift (δ) by ^{195}Pt NMR. The chemical shifts of ^{195}Pt were referenced to sodium hexachloroplatinate ($\delta = 0$ ppm). After incubation of CDDP3-encapsulated liposomes with chloride ion for 96 h, the chemical shift (δ) indicated only −2160 ppm, which is identical to the chemical shift (δ) of CDDP (Fig. 3). No chemical shift of CDDP3 ($\delta = -1620$ ppm) was detected indicating that CDDP3 in SLX liposomes efficiently converted to CDDP in the presence of chloride ions. The chemical shifts of −1620 ppm and −2160 ppm are consistent with those of CDDP3 and CDDP, respectively, as described by Rosenberg (1978).

3.2. Characterization of CDDP liposomes prepared from CDDP3

Encapsulation of CDDP in liposomes under various conditions was summarized in Table 1. When encapsulation was started with

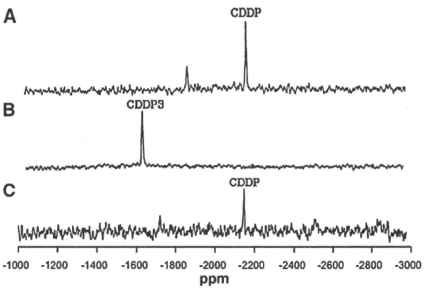

Fig. 3. Conversion of CDDP3 in the liposomes with SLX to CDDP detected by ^{195}Pt NMR. (A) 6.6 mM of CDDP in deuterium oxide; (B) 137 mM of CDDP3 in deuterium oxide; (C) CDDP3 encapsulated liposomes with SLX were treated with 150 mM NaCl for 96 h.

10 mg of CDDP3 and 4.5 mg of lipid, the resultant quantity of CDDP incorporated into SLX-Lip was 211 μg CDDP/3.5 mg lipid/mL and the loading efficiency was 6×10^{-2}. It is important to note that the quantity of CDDP in SLX-Lip increased from 211 μg to 821 μg depending on the amount of lipid. However, it was difficult to make the encapsulation efficiency higher than 10%. Since we found the loading efficiency was almost constant during the course of experiment, we took the loading efficiency as a parameter specific to the encapsulation method. On the other hand, the quantity of CDDP in SLX-Lip was 0.7 μg CDDP/3.5 mg lipid/mL and the loading efficiency was 2×10^{-3} when CDDP was directly encapsulated into liposomes. Actually 1.4 mg was the maximum amount of CDDP for encapsulation while 10 mg was available for CDDP3 in a similar condition. Thus, CDDP3 dramatically improved CDDP encapsulation by almost 300 times in quantity and 42 times in encapsulation efficiency when compared with direct encapsulation of CDDP into liposomes at the initial lipid amount of 4.5 mg. The CDDP loading efficiency appeared to be improved 30 times. The CDDP loading efficiency was improved by almost 4 times when compared with that of 1.4×10^{-2} for SPI-077 (Harrington et al., 2001; Kim et al., 2001). We successfully concentrated CDDP-SLX-Lip and CDDP-Lip up to 4.2 mg CDDP/70 mg lipid/mL, which was 20 times more than the concentration of CDDP in SPI-077. Dynamic laser scattering of the CDDP-SLX-Lip prepared from CDDP3 showed a mean diameter of about 160 nm (Table 1). The ζ potential of the liposomes was negative irrespective of the material of encapsulation (Table 1). Even after 6 months of storage at 4 °C, the leakage of CDDP from liposomes was only about 6% of the total amount of CDDP incorporated into liposomes just after preparation.

3.3. In vivo acute toxicity

The acute toxicity of CDDP-SLX-Lip was evaluated in normal mice by injection via tail veins. The mice were observed for 14 days after injection. The survival rate was 75% when mice received CDDP-SLX-Lip at doses of 18 or 25 mg CDDP/kg body weight. In contrast, the survival rates were 25% and 0% when mice received CDDP at doses of 18 and 25 mg CDDP/kg body weight, respectively (Fig. 4A). The mice did not die when they received empty liposomes with SLX. From these results encapsulation of CDDP in liposomes was found remarkably effective to protect mice from toxicity. This effect of encapsulation was not only recognized in the survival rate but also in the loss of body weight. When CDDP was administered at doses of 18 mg CDDP/kg body weight and 25 mg CDDP/kg body weight, the loss of body weight was 20% during 5 days and 25% during 4 days, respectively. The mice, which received CDDP-SLX-Lip at

Table 1
Physicochemical characteristics of CDDP liposomes prepared with CDDP or CDDP3 ($n = 3$).

	Method of encapsulation			
	I[a]	II[b]		
CDDP (mg)[c]	1.4	0	0	0
CDDP3 (mg)[c]	0	10	10	10
Lipid (mg)[c]	4.5	4.5	9	18
Lipid concentration (mg/mL)[d]	3.5 ± 0.4	3.5 ± 0.3	7.8 ± 0.5	16.5 ± 0.8
Particle size (nm)[e]	158 ± 6.5	150 ± 5.7	152 ± 5.5	160 ± 6.2
ζ potential (mV)	−57 ± 5.3	−55 ± 2.8	−50 ± 3.8	−54 ± 5.2
CDDP concentration (μg/mL)[f]	0.7 ± 0.2	211 ± 8	402 ± 0.5	821 ± 0.3
CDDP encapsulation efficiency (%)[g]	0.05	2.11	4.02	8.21
CDDP loading efficiency[h]	2×10^{-3}	6×10^{-2}	5×10^{-2}	5×10^{-2}

[a] Direct encapsulation of CDDP into liposomes.
[b] Encapsulation of CDDP3 into liposomes followed by conversion into CDDP in TAPS buffer containing NaCl.
[c] Initial amount used to prepare 1 mL of CDDP liposome.
[d] Total cholesterol in CDDP liposome solution was measured using a Determiner TC555 Kit.
[e] Measured by photon correlation spectroscopy with a Nano-S90 (Malvern). Polydispersity index was between 0.1 and 0.5 in each case.
[f] The amount of platinum was measured and the amount of CDDP was calculated as defined by Eq. (2) in Section 2.7.
[g] Encapsulation efficiency was calculated as defined by Eq. (3) in Section 2.7.
[h] Loading efficiency was calculated as defined by Eq. (4) in Section 2.7.

the dose of 18, 25 and 50 mg CDDP/kg body weight, showed the loss of body weight by about 15% during 3 days and recovered the loss by less than 10% during 5 days (Fig. 4B). Liposomes without CDDP had no significant effect on the body weight. These results support the possibility that CDDP-SLX-Lip can significantly reduce the toxicity of CDDP *in vivo*.

3.4. Effect of CDDP-SLX-Lip on normal tissues

The effect of CDDP-SLX-Lip and CDDP on normal tissues of mice was histologically evaluated (Fig. 5). Kidney, spleen and liver were excised from mice, which received a dose of 25 mg CDDP/kg body weight. Since mice died at day 4 from the injection of CDDP, tissues were prepared at day 4 after injection. Tissues were stained with HE and by TUNEL method to assess for apoptosis. Abnormal changes were not found in the kidney in mice which received both CDDP-SLX-Lip and CDDP (Fig. 5a,c) but TUNEL positive tubular epithelial cells were sporadically detected after CDDP treatment (Fig. 5d). CDDP-SLX-Lip treatment also did not produce any abnormal changes in the spleen (Fig. 5e,f). However, CDDP treatment of mice induced atrophy of the follicles with necrosis and a decrease in cell number in the white pulp (Fig. 5g). In follicles, phagocytosed dead lymphocytes were observed. TUNEL positive cells were also found in the white pulp (Fig. 5h). In liver, abnormal cells and TUNEL positive cells were not found after the administration of either CDDP-SLX-Lip (Fig. 5i,j) or CDDP (Fig. 5k,l).

3.5. Induction of E-selectin on HUVEC by EAT cells

Since SLX can bind to E-selectin, it is important to ascertain whether E-selectin expression occurs or can be induced on vascular endothelial cells in the tumor to validate tumor targeting. As shown in Fig. 6, E-selectin expression was induced on HUVEC, when stimulated by TNF-α. Although not all tumors may produce TNF-α, it is possible that tumors should express multiple cytokines, which can through a paracrine mechanism induce E-selectin expression on surrounding endothelial cells. The conditioned medium of EAT cells was in fact able to induce E-selectin expression on HUVEC in vitro while control medium did not (Fig. 6).

3.6. Expression of E-selectin on vascular endothelial walls in tumor

The thin section prepared from the solid EAT tissue was subjected to the assessment for the expression of E-selectin on vascular endothelial walls in the tumor. As shown in Fig. 7, E-selectin and blood vessels in the section were stained with anti-E-selectin antibody and LEL, which has specific affinity to fucose on the vascular endothelial cells. Since the sites of E-selectin expression agreed well with vascular walls, the vascular endothelial cells were judged to express E-selectin in the tumor tissue. These results as well as those in HUVEC suggest that the angiogenic vascular endothelial cells in EAT can be stimulated by cytokines or factors that are secreted from EAT cells to induce E-selectin expression.

3.7. Accumulation of CDDP in tumors

We previously reported that the accumulation of liposomes with SLX in the tumor was highest at 48 h after injection when evaluated by *in vivo* imaging using Cy5.5-encapsulated liposomes with SLX (Hirai et al., 2007a). On the basis of these data, the accumulation of CDDP-SLX-Lip in tumors was evaluated at 48 h after injection. CDDP-SLX-Lip or CDDP-Lip were independently administrated into the tail veins of mice bearing EAT tumors. The accumulation of CDDP in the tumors was evaluated by the amount of platinum derived from CDDP at 48 h after injection. The accumulation of CDDP from CDDP-SLX-Lip in the tumors was 6 times higher than that by CDDP-Lip indicating the potential targeting ability of CDDP-SLX-Lip *in vivo* (Fig. 8).

3.8. Antitumor effect of CDDP-SLX-Lip in vivo

The antitumor effect of CDDP-Lip and CDDP-SLX-Lip was evaluated in a mouse xenograft model of A549 lung carcinoma cells because CDDP is widely used for the treatment of lung carcinoma. When CDDP was administrated at 25 mg/kg body weight, all mice died at day 4 after injection. The volume of the tumors that were exposed to either CDDP-Lip or CDDP-SLX-Lip was significantly smaller than that of the non-treated tumors. A difference in tumor volumes between the two different CDDP containing liposomes could not be detected until 12 days after injection. CDDP-SLX-Lip suppressed the growth of tumors much more effectively than CDDP-Lip 19–26 days after injection. Suppression of tumor growth by CDDP-Lip (arrow a in Fig. 9) could be attributed to an enhanced permeability and retention effect (EPR). Further suppression induced by CDDP-SLX-Lip (arrow b in Fig. 9) might be accounted for by the effect of active targeting through the binding of SLX to the tumor vascular endothelial cells.

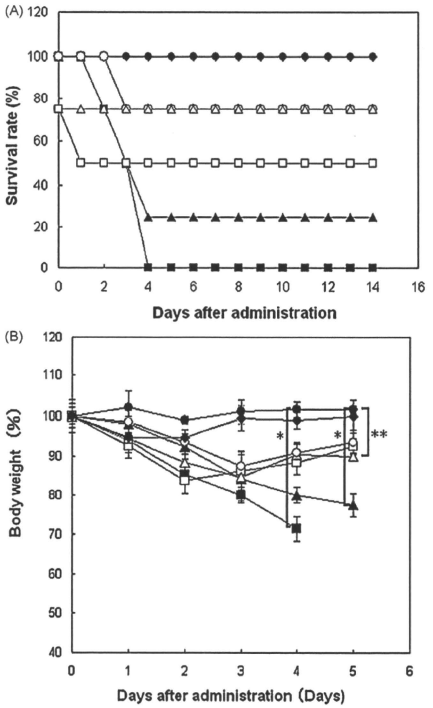

Fig. 4. Survival rate and body weight change of normal mice that received CDDP-SLX-Lip. (A) Survival rate (%); (B) body weight (%). Keys: ▲, CDDP solution (18 mg CDDP/kg body weight); ■, CDDP solution (25 mg CDDP/kg body weight); ○, CDDP-SLX-Lip (18 mg CDDP/kg body weight); △,CDDP-SLX-Lip (25 mg CDDP/kg body weight); □, CDDP-SLX-Lip (50 mg CDDP/kg body weight); ♦, empty liposomes; ●, saline solution. Each sample was injected into normal mice (female, 8 weeks) via tail veins. Results are expressed as the mean ($n = 4$); bars, ±SE. *$P < 0.005$; **not significant ($P > 0.05$).

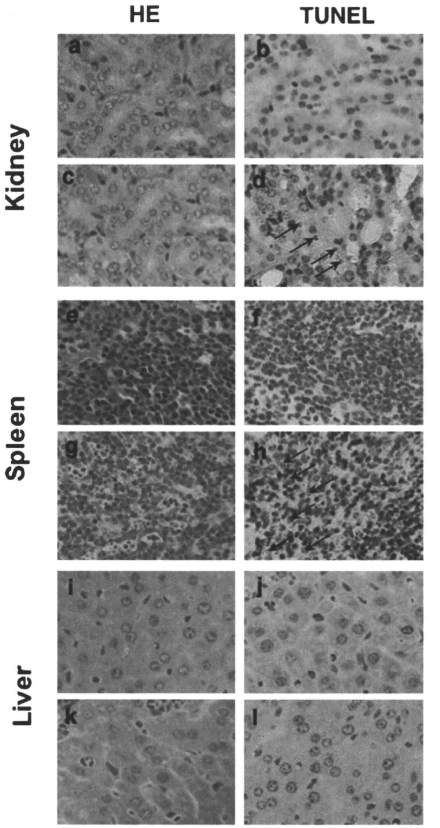

Fig. 5. Histochemical analysis of organs, which received CDDP and CDDP-SLX-Lip. CDDP-SLX-Lip (a, b, e, f, i, j) or CDDP (c, d, g, h, k, l) was injected into each normal mouse (Balb/c, female, 8-week-old) via tail veins at the dose of 25 mg CDDP/kg body weight. At 3 days after administration, kidney (a, b, c, d), spleen (e, f, g, h) and liver (i, j, k, l) were excised and fixed. HE staining (a, c, e, g, i and k) and TUNEL immunohistochemical staining (b, d, f, h, j and l) of the slices were observed. Black arrows indicate TUNEL positive cells. Objective lens was 60×.

4. Discussion

Here we have established a simple and novel method to encapsulate CDDP into liposomes at significantly high concentrations. We then applied this methodology to generate liposomes containing SLX to selectively target tumors and to substantially eliminate or reduce the deleterious and toxic side effects of high dose of CDDP. To achieve high concentrations of CDDP that could be encapsulated into liposomes, we chose to use CDDP3. Since CDDP3 is a hydrophilic derivative of CDDP and readily converts to CDDP in the presence of chloride ions (Fig. 1C), the entire encapsulation procedure could be executed in an aqueous phase. As shown in Fig. 2, CDDP3 was first dissolved at a saturated concentration in a buffer without chloride ions and encapsulated into liposomes. CDDP3 in the liposomes was then converted into CDDP by replacing buffer with buffer containing 150 mM NaCl. As the result, the CDDP encapsulation efficiency and the CDDP loading efficiency were drastically improved when compared with the conventional method of directly encapsulating CDDP. The CDDP loading efficiency in CDDP-SLX-Lip was improved by almost 4 times even when compared with the antecedent CDDP liposome, SPI-077 (Harrington et al., 2001; Kim et al., 2001). The amount of CDDP encapsulated in this study was considerably higher than could be accounted for by the enhanced solubility of CDDP3 in water as compared to CDDP. The negatively charged surface of the liposomes was designed to avoid being bound by blood proteins, such as opsonin, as well as to enhance the retention in blood. CDDP3 in aqueous solution is positively charged, so that it is conceivable that CDDP3 can be electrostatically bound to negatively charged lipids when encapsulated into liposomes.

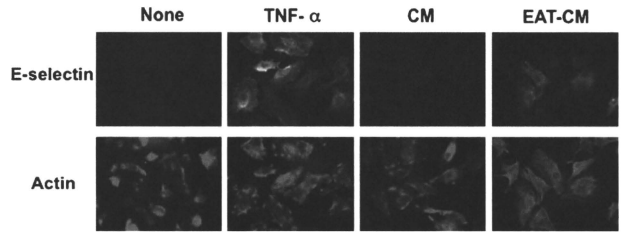

Fig. 6. Evaluation of E-selectin expressed on HUVEC. Cells were cultured in medium for HUVEC supplemented 10% FBS (None), or with 10 ng/mL of TNF-α (TNF-α), in DMEM supplemented 10% FBS (CM), or with EAT cultured DMEM supplemented 10% FBS (EAT-CM) for 4 h. To detect E-selectin, anti-E-selectin antibody was used followed by FITC labeled anti-mouse IgG polyclonal antibody (E-selectin). Actin filaments were stained with rhodamine labeled phalloidin (Actin). The magnification was 40×.

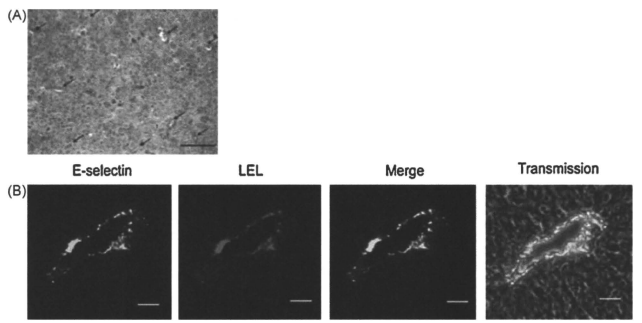

Fig. 7. The expression of E-selectin in vascular vessels of solid EAT. (A) HE staining of the section. Arrows indicated locations of vascular vessels. Scale bar: 100 μm. (B) Vascular vessel stained for E-selectin and for LEL. After deparaffinized, the section was incubated with anti-E-selectin antibody (10 μg/mL) for 1 h at 37 °C, then incubated with FITC labeled goat anti-mouse IgG and LEL conjugated with Texas red for 1 h at room temperature. Merge, colocalization of E-selectin and vascular endothelial cells was shown in yellow. Scale bar showed 20 μm.

The mean diameter of CDDP-SLX-Lip particle in the present study was about 160 nm (Table 1). Due to the SLX moiety, CDDP-SLX-Lip more than likely bind to the E-selectin on tumor vascular endothelial cells where they may enter the gaps between endothelial cells of the capillary bed, which are in the range of 100–300 nm and thereby penetrate into the tumor (Drummond et al., 1999; Gabizon, 1992; Huang et al., 1992, 1993; Wu et al., 1993).

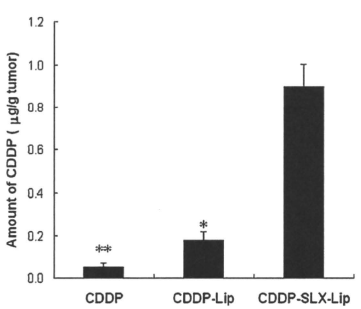

Fig. 8. Accumulation of CDDP in the tumor in vivo. At day 10 after transplantation of EAT cells, CDDP-SLX-Lip, CDDP-Lip or CDDP (2 mg/kg body weight as CDDP) were administered from tail veins of mice. At 48 h after injection the tumor tissues were excised and the amount of platinum were measured by FAAS. Results are expressed as the mean ± SD ($n = 3$). *$P < 0.01$ compared with CDDP-Lip. **$P < 0.005$ compared with CDDP.

CDDP-SLX-Lip were evaluated *in vivo* for acute toxicity and antitumor activity with target potential. The acute toxicity of CDDP was apparently and remarkably reduced by the encapsulation of CDDP in SLX liposomes. When CDDP was injected at 25 mg CDDP/kg body weight, significant toxicity in the kidney was not obvious by HE staining (Fig. 5c) and the TUNEL assay showed only a small number of positive cells in kidney (Fig. 5d). In this part of the study, the period between administration of CDDP and removal of tissues was 3 days, which was probably too short for CDDP to exhibit any significant nephrotoxicity. To observe more dramatic nephrotoxic effects of CDDP, it would probably require longer periods of administration at lower doses of CDDP. As for the acute toxicity, we can conclude that CDDP-SLX-Lip are relatively safe as drug when compared to CDDP with an excellent survival rate as shown in Fig. 4. It is noteworthy that CDDP-SLX-Lip loading of 25 mg CDDP/kg body weight showed significant antitumor activity in vivo (Fig. 9). While an EPR effect should allow the accumulation of CDDP-Lip in tumors (Matsumura and Maeda, 1986) active targeting by CDDP-SLX-Lip exhibited an additive effect. In this context, CDDP-SLX-Lip were more effective than CDDP-Lip at 19 and 26 days after administration (Fig. 9). The accentuated antitumor activity appearing in the late stages may be related to leakage of CDDP from CDDP-SLX-Lip into the tumor. Furthermore, the expression of E-selectin on tumor vascular endothelial cells may be upregulated by tumor-